TISSUE ENGINEERING
Volume 12, Number 2, 2006
© Mary Ann Liebert, Inc.

Biomimicking Extracellular Matrix: Cell Adhesive RGD Peptide Modified Electrospun Poly(D,L-lactic-co-glycolic acid) Nanofiber Mesh

TAEK GYOUNG KIM, M.S. and TAE GWAN PARK, Ph.D.

ABSTRACT

A cell adhesive peptide, Arg-Gly-Asp (RGD), was immobilized onto the surface of electrospun poly(D,L-lactic-co-glycolic acid) PLGA nanofiber mesh in an attempt to mimic an extracellular matrix structure. A blend mixture of PLGA and PLGA-*b*-PEG-NH_2 di-block copolymer dissolved in a 1:1 volume mixture of dimethylformamide and tetrahydrofuran was electrospun to produce a nanofiber mesh with functional primary amino groups on the surface. Various electrospinning parameters, such as polymer concentration and the blend ratio, were optimized to produce a nanofiber mesh with desirable morphology, surface characteristics, and fiber diameter. A cell adhesive peptide, GRGDY, was covalently grafted onto the aminated surface of the electrospun mesh under a hydrating condition. The amounts of surface primary amino groups and grafted RGD peptides were quantitatively determined. Cell attachment, spreading, and proliferation were greatly enhanced in the RGD modified electrospun PLGA nanofiber mesh compared with that of the unmodified one.

INTRODUCTION

EXTRACELLULAR MATRIX (ECM) provides cells or tissues with structural integrity and biofunctional contacting surface. Morphological and surface designs of synthetic polymeric biomaterials involving tissue regeneration and treatment of wounds have been focused on biomimicking natural ECM environments.[1,2] These bio-inspired biomaterials are expected to induce cellular responses, such as adhesion, proliferation, migration, and differentiation, as the natural ECM does. Micro- or nanotopographic pattern formation on the surface of biomaterials controls cellular behaviors to varying extents.[3,4] ECM consists of an ill-defined, amorphous association of proteins and polysaccharides, which interact together to form an interconnected nano- or microranged fibrous network that is bound to the surface of cells.[5] Among the components, collagens are abundant fibrous proteins providing the ECM with high mechanical strength and, more importantly, have many cell adhesive peptide moieties for anchoring the cells. Thus, ECM bio-inspired biomaterials have been fabricated by biomimicking the fibrous and interconnected ECM structure.

Recently, an electrospinning technique has received much attention for fabricating polymeric ultrafine nanofibers. The electrospinning is a facile, efficient, and inexpensive polymer processing method for the formation of nonwoven fabrics, in which a polymer solution dissolved in a solvent is ejected through a nozzle by an electrostatic force. When high voltage is applied, electrostatic charge is induced on the surface of the polymer solution droplet. As the electric field reaches a critical value, mutual charge repulsion and coulombic force exerted by the external electric field counteract the surface tension of the droplet, generating a charged jet stream of polymer solution. The jet stream becomes very thin and long through an unstable elongation process. During the electrospinning, the solvent evaporates and the charged

Department of Biological Sciences, Korea Advanced Institute of Science and Technology, Daejeon, South Korea.

polymer nanofibers are deposited on a grounded collector.[6] The resultant structure is a three-dimensional, randomly oriented nanofiber network mesh with a highly nano-porous architecture. The structure resembles the collagen fiber network existing in the natural ECM. In native tissues, the diameter of collagen fibrils range from 30 to 300 nm.[7] However, electrospun nanofibers with a diameter in the range of 300 to 1000 nm also provide an appropriate environment for cell attachment, proliferation, and migration that is as good as that in the natural ECM.[8–10] Thus, a wide range of electrospun biodegradable nanofibers with larger diameters than natural collagen fibrils have been used for temporal scaffolds for regeneration of tissues.[11,12]

Synthetic biodegradable polymers, such as poly(ε-caprolactone), poly(L-lactic acid), and their copolymers with D-lactic or glycolic acid, have been extensively used for fabrication of temporal porous scaffolds due to their controllable biodegradability and proven biocompatibility.[13,14] In our previous studies, porous poly(D,L-lactic-co-glycolic acid) (PLGA) biodegradable scaffolds were fabricated using a novel salt-leaching/gas-foaming method.[15] While they showed good tissue-forming abilities, it is highly desirable to fabricate porous scaffolds made of biodegradable polymeric nanofibers. In this scaffold structure, the inner pores, where the cells will reside, would be surrounded by a network structure of nanofibers, mimicking the ECM structure.

A tri-amino acid peptide, Arg-Gly-Asp (RGD), is the best known peptide sequence for prompting cell adhesion on synthetic material surfaces. The RGD sequence is a cell recognition motif found in many ECM proteins such as collagen, laminin, fibrinogen, and vitronectin that bind to integrin receptors.[16] The cellular interactions with ECM through integrin-mediated binding promote specific cellular behaviors such as cell attachment, spreading, and formation of focal adhesions.[17] Moreover, the cell adhesion mediated by integrin receptors enhances viability and proliferation of anchorage dependent cells.[18] In many previous studies, a wide range of polymeric biomaterials, of which the surface was modified with RGD moieties, have been used for modulating cellular behaviors, such as adhesion, migration, and differentiation.[19–21]

In this study, we are interested in preparing ECM mimicking PLGA nanofiber mesh with cell adhesive RGD moieties on the surface, prior to fabricating the three-dimensional porous nanofiber scaffolds. A blend mixture of PLGA and PLGA-*b*-PEG-NH_2 di-block copolymer was electrospun to produce PLGA nanofiber mesh with primary amino groups on the surface. The di-block copolymer with a primary amino group at the PEG end served as a surface-modifying agent that made the primary amino groups exposed on the surface of nanofibers under hydrating conditions. Various electrospinning parameters, such as polymer concentration and blend weight ratios, were scrutinized to optimize the formation of PLGA nanofibers. The resulting electrospun nanofiber mesh was characterized by measuring the change of water contact angle and by determining the surface amine concentration. A cell adhesive Gly-Arg-Gly-Asp-Tyr (GRGDY) peptide was immobilized on the surface of aminated nanofiber mesh, and the surface RGD concentration was determined. Using the RGD-modified PLGA nanofiber mesh, cell adhesion and proliferation behaviors were studied using NIH3T3 fibroblast cells.

MATERIALS AND METHODS

Poly(D,L-lactic-co-glycolic acid) (lactic-glycolic acid ratio 75:25, RG756, Mw 100,000) and PLGA (lactic-glycolic acid ratio 50:50, RG504H, Mw 45,000) were purchased from Boehringer Ingelheim (Ingelheim, Germany). Unless otherwise noted, standard laboratory chemicals were purchased from Sigma-Aldrich (St. Louis, MO).

Preparation of amine terminated PEG-b-PLGA di-block copolymers

PLGA-*b*-PEG-NH_2 was prepared using RG504H (PLGA) according to the method previously reported.[22] Synthesis of the di-block copolymer was confirmed by ^{1}H-NMR and differential scanning calorimetry.

Fabrication of aminated PLGA meshes via electrospinning

The electrospinning apparatus was constructed based on our previous studies.[23,24] A blend mixture of PLGA (RG756) and PLGA-*b*-PEG-NH_2 was dissolved in a mixed solvent of *N,N*-dimethyl formamide (DMF) and tetrahydrofuran (THF) (1:1 v/v). The composition and concentration of the polymer solution are listed in Table 1. For electrospinning, each polymer solution was placed in a horizontally fixed 5 mL glass syringe with a 23 gauge stainless steel needle. The polymer solution was delivered to the needle by a syringe pump (model 210, KD Scientific, Holliston, MA) at a constant feed rate of 20 μL/min. An 18 kV positive voltage was applied to the metal needle using a high-voltage DC power supply (CPS-40 K03VIT, Chungpa EMT, Seoul, Korea). Randomly oriented fibrous mesh was collected on a grounded rotating drum (wrapped with aluminum foil), positioned 18 cm from the needle. The resulting PLGA meshes were placed in a vacuum oven to remove residual solvent for 3 days. All procedures were carried out under ambient conditions.

Characterization

Prior to electrospinning, viscosity values of the polymer solutions with various blend ratios were measured

Table 1. Spinning Solution Viscosities and Average Fiber Diameters of Electrospun Fiber Meshes Prepared with Different Polymer Solutions

Formulation	*PLGA/PLGA-b-PEG-NH_2 (w/w)*	*Concentration (% w/v)*	*Spinning solution viscosity (cP)*	*Average fiber diameter (nm)*
#1	100/0	30	1261	761 ± 120
#2	90/10	30	732	615 ± 163
#3	80/20	30	383	453 ± 149
#4	70/30	30	220	449 ± 150
#5	70/30	40	—	726 ± 260
#6	70/30	50	—	1312 ± 292

with an advanced rheometric expansion system (ARES, Rheometric Scientific, Piscataway, NJ) using a cone and plate geometry. A steady rate sweep test was performed to the polymer blend solutions at 25°C. The morphology of the electrospun mesh was examined with scanning electron microscopy (SEM, Philips 535M, Eindhoven, the Netherlands) after sputter-coated with gold particles. From the SEM pictures, the fiber diameter was determined by using an image analyzer[25] (Image J, developed by the U.S. National Institute of Health) (100 nanofibers in 3 different pictures were used in calculating the average diameter). The amount of primary amino group on the surface of aminated PLGA mesh was determined by using a coupling reaction of an amine reactive fluorescamine dye with the primary amino group. Briefly, the mesh (10 mg) was pre-wetted with 70% ethanol and washed with doubly distilled water successively. To fully expose the hydrophilic block of PEG-NH_2 in the di-block copolymer on the surface, the mesh was hydrated in phosphate buffered saline (PBS, pH 7.4) solution for 24 h at room temperature. Subsequently, the mesh was soaked in 3 mL of 50 mM borate buffer (pH 9) containing 300 μL fluorescamine solution (0.3 mg/mL in acetone) for 5 min with vortexing and 15 min with gentle shaking. The resulting yellowish mesh was washed with methanol and observed by using laser scanning confocal microscope (LSCM, Carl Zeiss LSM5100, Jena, Germany). To quantify the surface amine concentration, the fluorescamine-conjugated mesh was dissolved in 1 mL of dimethylsulfoxide (DMSO). Fluorescence intensity of the polymer solution was measured by a spectrofluorophotometer (RF-5391PC, Shimadzu, Kyoto, Japan) at 390 nm of excitation wavelength and 475 nm of emission wavelength. The amount of surface amino group was then calculated from a calibration curve, which was constructed by using PEG di-amine and PLGA dissolved in DMSO.

RGD peptide grafting

For the surface coupling reaction with GRGDY peptide (Peptron, Daejeon, Korea), aminated PLGA meshes (30:70 weight ratio of PLGA-b-PEG-NH_2 and PLGA) with various fiber diameters were pre-wetted and hydrated as described above. The reaction scheme for peptide coupling was followed as previously reported.[22] Briefly, each mesh (10 mg) was immersed in 2 mL PBS containing 60 nmol ethylene glycol-bis(sulfosuccinimidylsuccinate) (EGS, Pierce Biotechnology, Rockford, IL) with gentle agitation for 1 h at room temperature. After rinsing with PBS, the NHS-activated mesh was put into 2 mL PBS containing 15 μg GRGDY peptide under shaking for 24 h at room temperature. At the end of the coupling reaction, the peptide-immobilized mesh was rinsed in PBS and doubly distilled water, and then lyophilized. The amount of immobilized GRGDY peptide on the mesh surface was determined using a colorimetric ninhydrin method.[20] The RGD immobilized mesh was put into a mixture of 1 mL of 5 N HCl and 4 mL PBS, heated at 120°C for 10 min, and then cooled for 1 h at room temperature. An aliquot (1 mL) from the resultant solution was neutralized with 4 N NaOH, followed by addition of ninhydrin reagent solution (0.2 mL). The solution was heated at 100°C for 5 min, to ensure complete color development, and cooled to room temperature, followed by adding 5 ml of 50% ethanol. The amount of RGD peptide was determined by using UV spectrophotometry (UV-1601, Shimadzu) at 570 nm. A standard calibration curve was constructed by using the aminated PLGA mesh and a known amount of GRGDY peptide.

Wettabililty of electrospun mesh

Water contact angles of PLGA, aminated PLGA before and after hydration, and RGD-modified PLGA meshes were measured using a contact angle measurement system (SEO 300A, SEO, Gunpo, Korea) mounted with a CCD camera at an ambient condition. The contact angle variation of a water drop was evaluated as a function of time,[26] since the water drop was rapidly infiltrated into the aminated mesh. The $12 \times 12 \times 0.2$ mm mesh was carefully placed on a sample stage, and a single drop of doubly distilled water was applied to the mesh surface. The images were taken at a rate of 60 frame/min.

Analysis of cell attachment

NIH3T3 fibroblasts (the Korean Cell Line Bank, Korea) were maintained in 175-cm^2 tissue culture flasks (BD Sciences, San Jose, CA) at 37°C in a humidified 5% CO_2 environmental incubator. Culture medium consisted of Dulbecco's modified Eagle's medium (DMEM, Grand Island, NY) supplemented with 10% (v/v) FBS, 100 U/mL penicillin, and 100 g/mL streptomycin. To prepare cell suspensions, the cultured cells were harvested using trypsin/EDTA, centrifuged at 1000 rpm for 5 min, and resuspended in serum-free DMEM. Each electrospun mesh (12 × 12 mm) was sterilized by UV irradiation for 2 h and 70% ethanol for 12 h, and then ethanol was exchanged with excess amount of deionized water and PBS. Subsequently, the mesh was placed into 16-well culture plates (BD Sciences), and cell suspensions were inoculated onto the mesh at 1×10^5 cell/cm^2 of cell-seeding density in a total of 2 mL of medium per well. After seeding, samples were incubated undisturbed in serum-free medium for 1, 2, 4, and 8 h. At each time point, cell/mesh constructs were harvested, washed in PBS three times to remove nonadherent and loosely attached cells, and placed into fresh culture medium, including cell counting kit-8 solution (CCK-8, Dojindo, Japan), which generated an orange formazan product by cellular dehydrogenases.[27] After incubating the cells with CCK-8 agent for 2 h, 100 μl of each sample was transferred to a 96-well plate, followed by measuring the absorbance at 450 nm in a microplate reader (Model 550, Bio-Rad, Hercules, CA). Cell number was calculated from a calibration curve obtained from the wells that contained a known number of viable cells.

Cell spreading

For the observation of morphological change with the passage of time, the cell/mesh constructs were harvested at 2 and 8 h, rinsed with warm PBS, and fixed with 3.7% glutaraldehyde for 12 h at 4°C. After dehydration through a series of graded ethanol (50, 70, 90, and 100%), each cell/mesh construct was dried under a laminar air flow for 1 day. Scanning electron microscopy was employed to examine cell spreading. For the measurement of the cell-spreading area, the cells incubated for 2 h were stained with a Cell Tracker Orange dye (Molecular Probes, Eugene, OR).[28] One hundred cells from five images of different regions were analyzed by Image J software. In order to visualize actin filaments, the cells attached on the mesh were stained with rhodamine phalloidin (Molecular Probes) according to the manufacturer's instruction. Briefly, cell-polymer constructs were washed twice with prewarmed PBS solution. Then they were fixed for 20 min with 3.7% formaldehyde in 1% Triton X-100 solution, followed by staining with 0.2 μM rhodamine-phalloidin for 30 min. After washing, F actin-labeled cells were photographed by using a Carl Zeiss LSM5100 confocal microscopy.

Cell proliferation

Each sterilized electrospun mesh was placed into a 16-well culture plate. NIH 3T3 cells were seeded with a cell density of 1×10^4 cell/cm^2. After attaching fibroblasts in serum-free conditions, each mesh was placed and incubated in DMEM containing serum for 5 days. Culture medium was replaced with fresh medium every day. Cell numbers at 1, 3, and 5 days were counted by using CCK-8 solution. At 5 days, cellular constructs were observed by scanning electron microscopy.

Statistical analysis

Data were expressed as a mean ± standard deviation (SD). Student's *t* test analysis was carried out for the cell proliferation data of aminated and RGD-immobilized mesh. Significance was determined at $p < 0.05$.

RESULTS

Characterizations of electrospun fiber mesh

Both electrospun PLGA and aminated PLGA fiber meshes showed a nonwoven, bead-free, linear, porous, and partially interconnected fibrous structure (Fig. 1). Significant change in fiber diameter occurred upon varying the blend composition and concentration of the polymer solution. As shown in Table 1, the average diameter of electrospun fibers increased with the concentration of polymer solution at a constant blend ratio. The fiber diameter in general is highly dependent on the viscosity of spinning polymer solution. The viscosity was regarded as a key parameter in the formation of nanofibers by the electrospinning process, as shown previously.[29] When the blend ratio of PLGA-*b*-PEG-NH_2 block copolymer to PLGA was increased, fiber diameters decreased as a result of reduced viscosity values. At a blend ratio above 30% (w/w), a bead-on-string structure was obtained (data not shown), indicating an unstable fibrous structure was produced. The electrospun meshes with various polymer concentrations were prepared in order to investigate the effect of fiber diameter on the surface amine concentration. At a fixed blend ratio and a decreased diameter of nanofiber, the measured surface amine concentration increased from 0.65 to 1.17 nmol/mg mesh (Fig. 2B). In the case of the nanofiber with a larger diameter, it is obvious that the amine functional group is more likely to be embedded inside the fiber, with little being exposed on the surface. With a smaller fiber diameter, surface area will significantly increase, causing embedded amino groups to be present on the outer surface. Figure 2A shows confocal image of the fibrous mesh conjugated

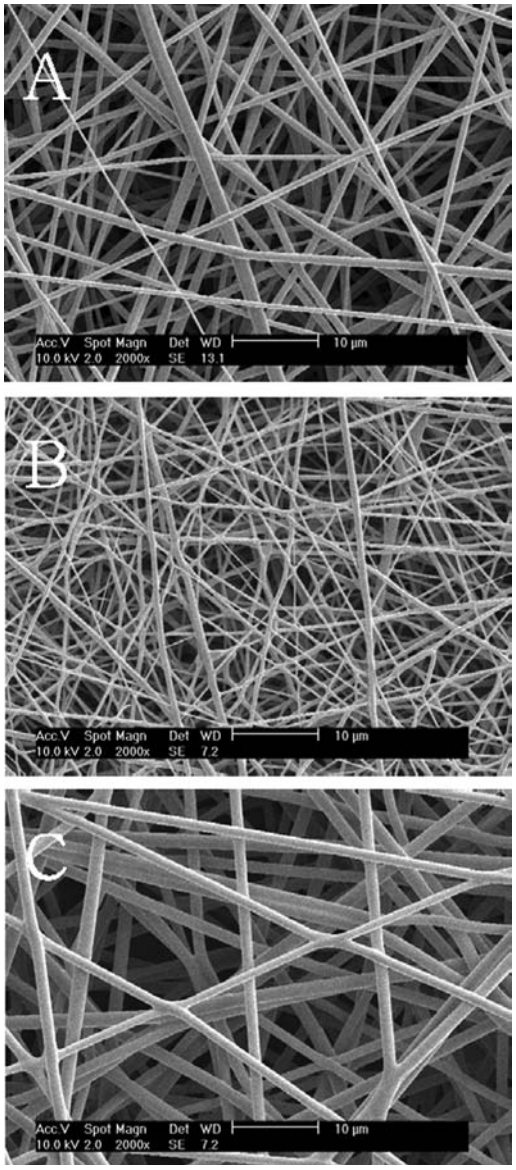

FIG. 1. SEM photographs of electrospun nanofibrous meshes. (**A**) Pure PLGA mesh at 30% (w/v) polymer concentration. (**B**) 30% (PLGA-b-PEG-NH_2/PLGA w/w) blend mesh at 30% (w/v) polymer concentration. (**C**) 30% (PLGA-b-PEG-NH_2/PLGA w/w) blend mesh at 50% (w/v) polymer concentration.

with an amine specific dye. The fluorescamine dye reacts only with primary amino groups, so the confocal image proved the presence of amino groups on the surface with a homogeneous distribution.

RGD immobilization and wettabililty

In this study, GRGDY peptide was used to immobilize to the NHS-activated PLGA mesh surface. In Figure 3, it can be seen that the amount of RGD peptide immobilized on the surface increased with increased blend ratio. Obviously, the higher blend ratio of PLGA-*b*-PEG-NH_2 di-block copolymer to PLGA resulted in the greater surface amine concentration, providing more sites for RGD peptide grafting on the surface. The blending PLGA-*b*-PEG-NH_2 di-block copolymer with PLGA was found to increase the surface wettability (Fig. 4). Initial water contact angle values for different meshes of PLGA, aminated PLGA before and after hydration, and RGD-modified meshes were 94, 87, 68.4, and 67.6°, respectively. The temporal ability of the electrospun fibrous mesh to retain a convex shape of a water drop primarily depends on its surface topography and chemical composition.[30] Since the mesh surface was porous and rough, a static water contact angle was not directly applicable for evaluating the surface wettability. During the test, the water sessile drop was rapidly imbibed into the aminated

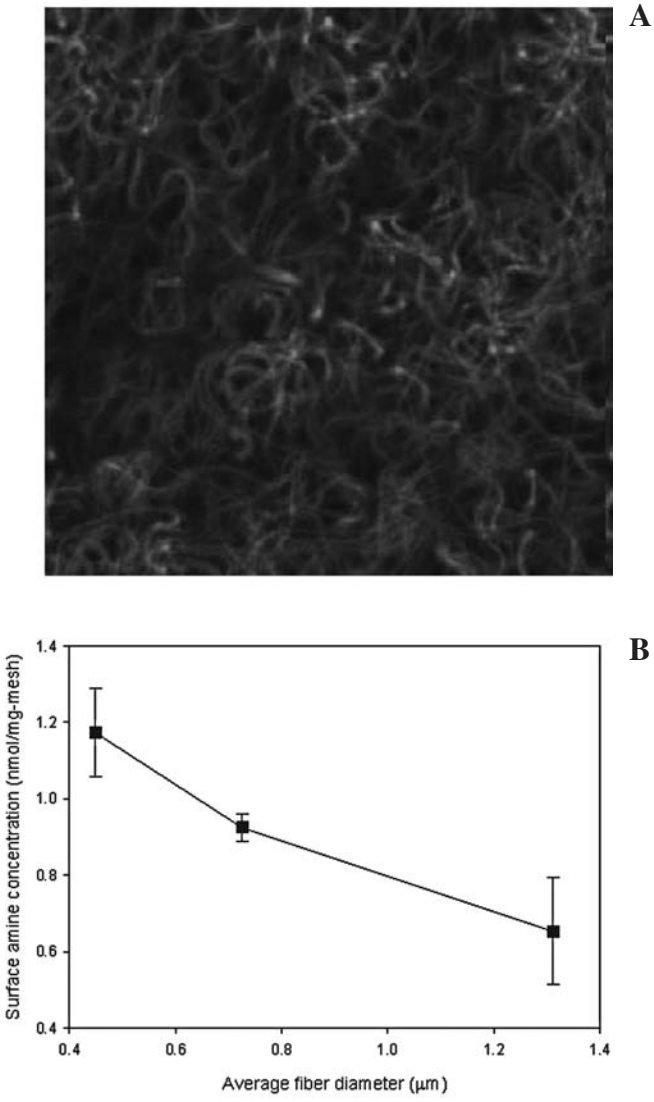

FIG. 2. (**A**) LSCM image of aminated PLGA mesh stained with amine reactive fluorescent dye (fluorescamine). (**B**) Surface amine concentration on fibers with different diameters.

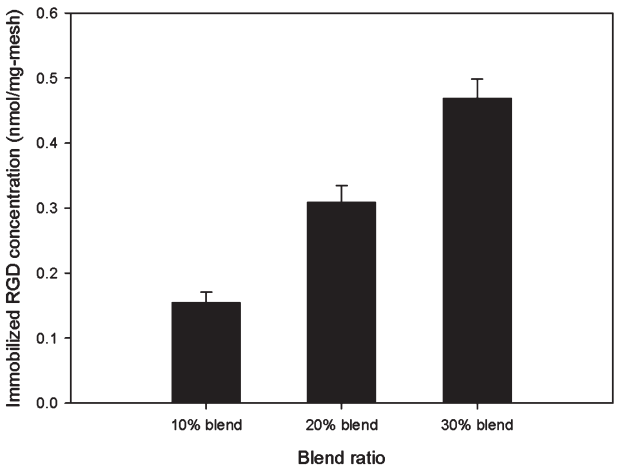

FIG. 3. Surface amine concentration as a function of blend ratio.

fibrous mesh, due to the hydrophilic nature of the PEGylated surface. The water drop on the aminated PLGA mesh can rapidly penetrate the pores to fill the void space within 17 s, while the drop on the surface of pure PLGA mesh maintained the shape to the end of the test. It was found that the water penetration time became shorter for the mesh when hydrated. This suggested that changes in surface properties, such as surface roughness and composition, occurred after hydration. PLGA-*b*-PEG-NH_2 di-block copolymer has an amphiphilic nature consisting of a hydrophobic PLGA part and a hydrophilic PEG part. The hydration induced the di-block copolymer to molecularly migrate and rearrange near the surface, exposing the hydrophilic PEG block to a water phase. Change of surface morphology after hydration was also observed visually. The water contact angle change of RGD immobilized mesh was found to be nearly the same as that of aminated PLGA mesh.

Cell adhesion, spreading, and morphology

Adhesion and spreading behaviors of NIH3T3 fibroblasts were examined for each nanofibrous mesh (PLGA, aminated, and RGD modified) in the serum-free medium. Figure 5 reveals that cellular adhesions onto both aminated and RGD-modified meshes were enhanced as compared with those of unmodified PLGA mesh. In addition, it was found that RGD-modified mesh showed the greatest cell adhesion efficiency. This clearly implied that the fibroblast adhesion occurred preferentially for the RGD-modified mesh. The initial cell attachment to the RGD-modified mesh was significantly promoted, relative to the other two meshes, by up to 8 h. At 8 h, fibroblast cells were robust and almost fully adhered to RGD-modified mesh (96%). However, the attachment efficiencies of PLGA and aminated PLGA meshes were 67 and 82%, respectively, after the same period.

Figure 6 provides visual comparisons of cell adhesion and proliferation for PLGA and RGD-modified meshes after 2 h, 8 h, and 5 days. Spreading rates of the cells for RGD-modified mesh was evidently increased, exhibiting a larger cell-spreading area. After 2 h incubation, cell morphology onto PLGA mesh was still round-shaped while the cells on RGD-modified mesh started to show spreading behaviors. Interestingly, it was observed that the fibers on the mesh surface were contracted and entangled above the cells, indicating that the cells tended to migrate and infiltrate into the interior of the mesh af-

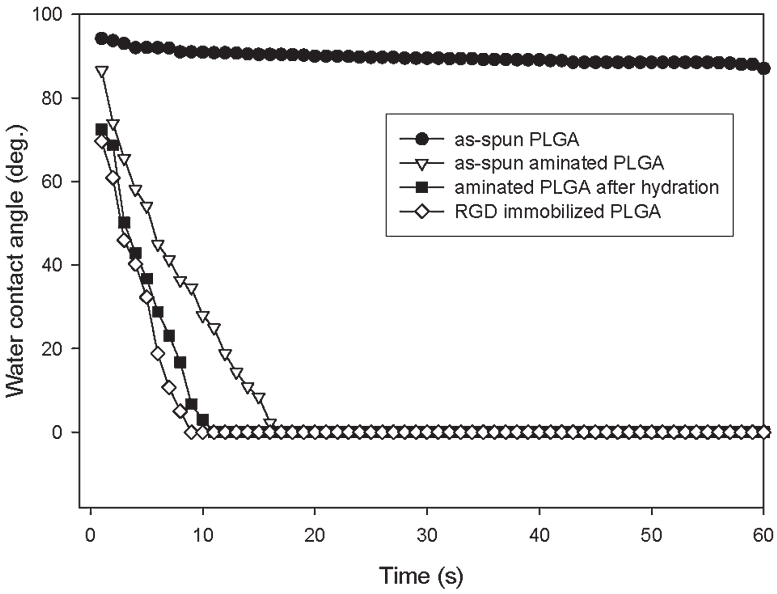

FIG. 4. Change in water contact angles of different electrospun fibrous meshes as a function of time.

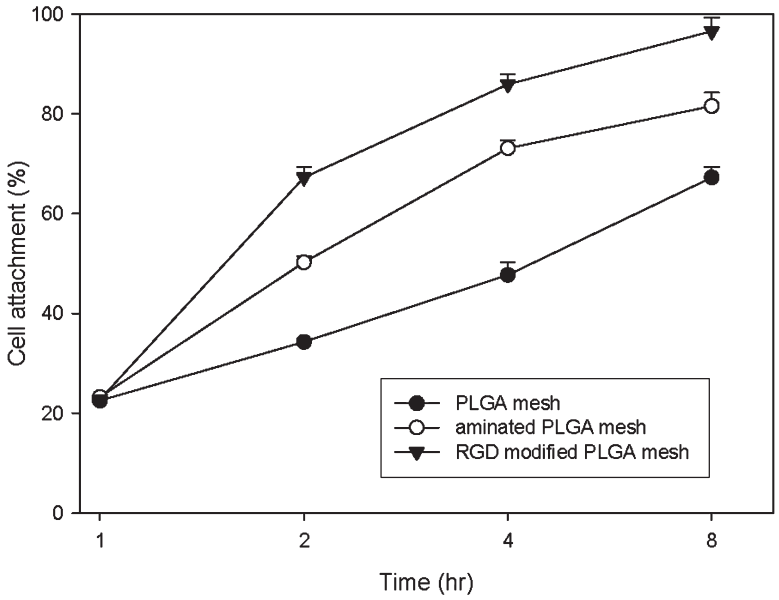

FIG. 5. Initial cell attachment kinetics for PLGA mesh, aminated PLGA mesh, and RGD-immobilized PLGA mesh.

ter 8 h. At day 5, the cells reached a confluence state and formed a monolayer on the surface. After 2 h of cell culture, LSCM images of cell/mesh constructs after staining by CellTracker probe (Molecular Probes, Eugene, OR) were used to calculate the cell-spreading area (Fig. 7A and B). Figure 8 shows the distribution of cell-spreading areas, clearly demonstrating that the attached cells were more spread out on the RGD-modified mesh. Actin stress fibers were qualified by rhodamine phalloidin staining (Fig. 7C and D). The result is consistent with the previous image that the cells on RGD-modified mesh were extensively spread.

Cell proliferation

Proliferations of NIH3T3 fibroblasts on the three meshes were evaluated at 1, 3, and 5 days (Fig. 9). The number of cells increased with time, suggesting that the cells proliferated well on the surfaces of all the meshes. The cell proliferation on RGD-immobilized nanofibers was significantly different from that on PLGA and aminated PLGA nanofiber meshes ($p < 0.05$) in early incubation period. However, at day 5, the cell proliferations on all the substrates were not significantly different. After day 5, the cell proliferation began to level off, meaning that the cells were in a confluence state, presumably by a contact inhibition mechanism.[31]

DISCUSSION

In this study, we successfully fabricated RGD-immobilized electrospun nanofibrous mesh useful for cell adhesive scaffolds, wound dressing materials, and prosthetic devices. The electrospinning of a blend mixture of PLGA-*b*-PEG-NH_2 and PLGA produced a highly porous nanofiber-based structure, which also has a large surface area, flexibility for surface modification, and sufficient mechanical strength for handling.[32] In the electrospinning process, various parameters, such as viscosity and surface tension of polymer solution, polymer molecular weight, applied electrical potential, and the distance between the needle and the collector, determine the resultant fibrous morphology and diameter.[6,33] In the present study, a slight change in the viscosity of polymer solution by adjusting the polymer concentration and the blend ratio primarily produced different fiber diameters. As described elsewhere, the results showed the decrease in viscosity made the fiber diameter smaller. Since we intended to produce the nanofibrous mesh exposing more surface functional groups, a stable nanofibrous structure with a smaller fiber diameter was produced for the RGD immobilization. The aminated PLGA nanofibrous mesh with 30% (w/w) of PLGA-*b*-PEG-NH_2/PLGA blend ratio and 449 nm of average fiber diameter was chosen for the subsequent RGD grafting experiment.

In previous studies, electrospun nanofibrous PLGA matrices exhibited favorable cell-polymer interactions.[8] The fibrous architecture mimicked the natural extracellular matrix and assisted the cells in maintaining a phenotypic shape. Surface topography plays a critical role in regulating initial cell behaviors, such as cell adhesion and spreading events, which can also influence cellular viability and differentiation in a later stage.[34,35] There is abundant evidence that cells respond to topographical

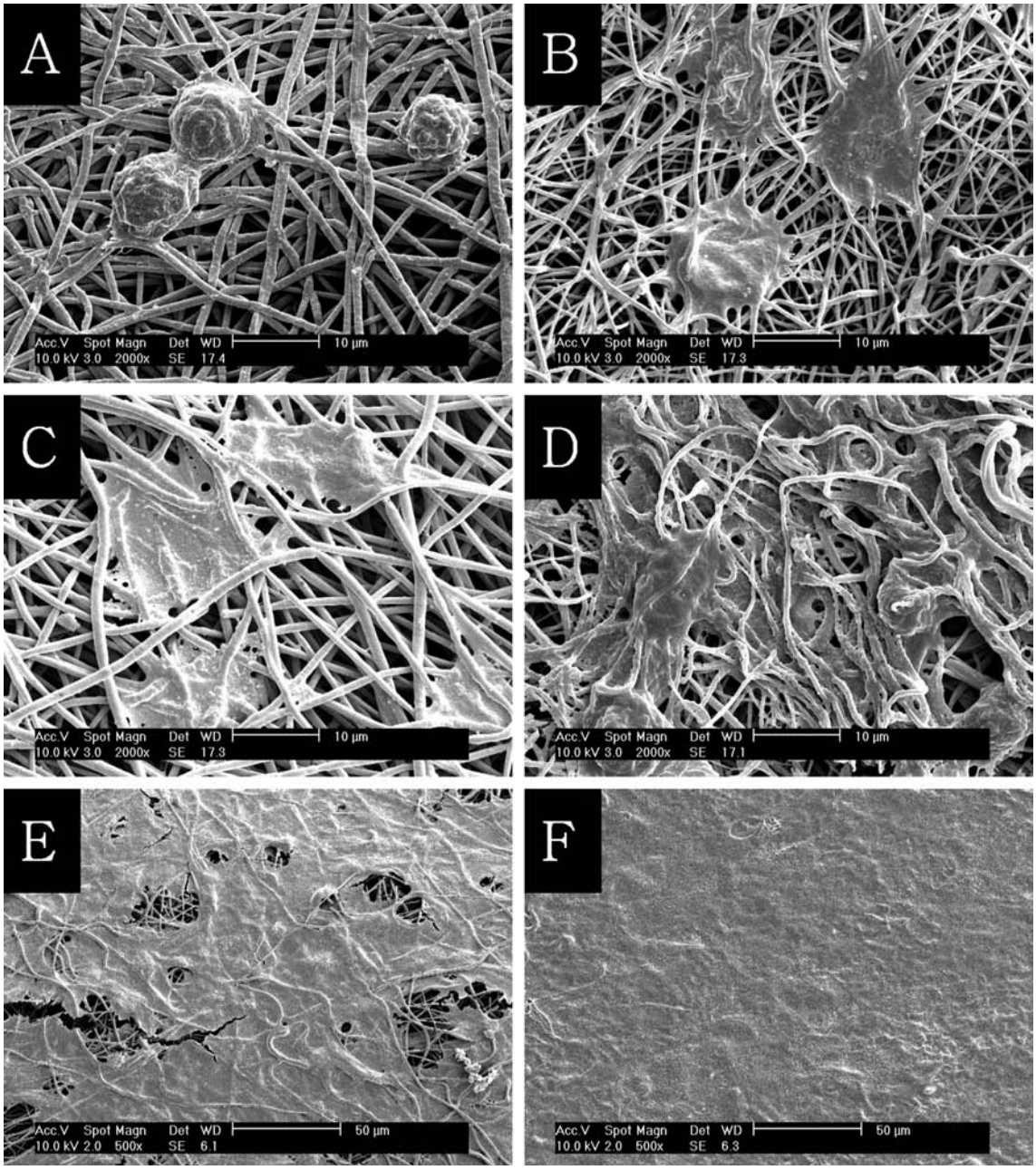

FIG. 6. SEM images of cellular constructs. **(A, C, and E)** PLGA mesh at 2 h, 8 h, and 5 days, respectively. (**B, D, and F**) RGD-immobilized PLGA mesh at 2 h, 8 h, and 5 days, respectively.

discontinuities with patterns of grooves and ridges.[36] Therefore, it is expected that a texture structure of electrospun nanofibrous mesh can control temporal and spatial organization of adhered cells. A previous work showed that cell adhesion is cooperatively regulated by the matrix topography and the presence of cell recognition ligands on the surface.[34] It was suggested that cellular responses to the topographic structure would depend on size scale and geometric features, as well as the local density of surface ligands. To mimic surface properties of synthetic biomaterials to a set of predetermined biological microenvironments, cell adhesive proteins like collagen, fibronectin, and laminin have been coated on the surface of biomaterials.[37,38] Nonetheless, the chemical conjugation of small RGD moieties on the surface was more advantageous than the protein-coating method for controlling cell adhesion behaviors, because the surface immobilization of cell adhesive ligands affords

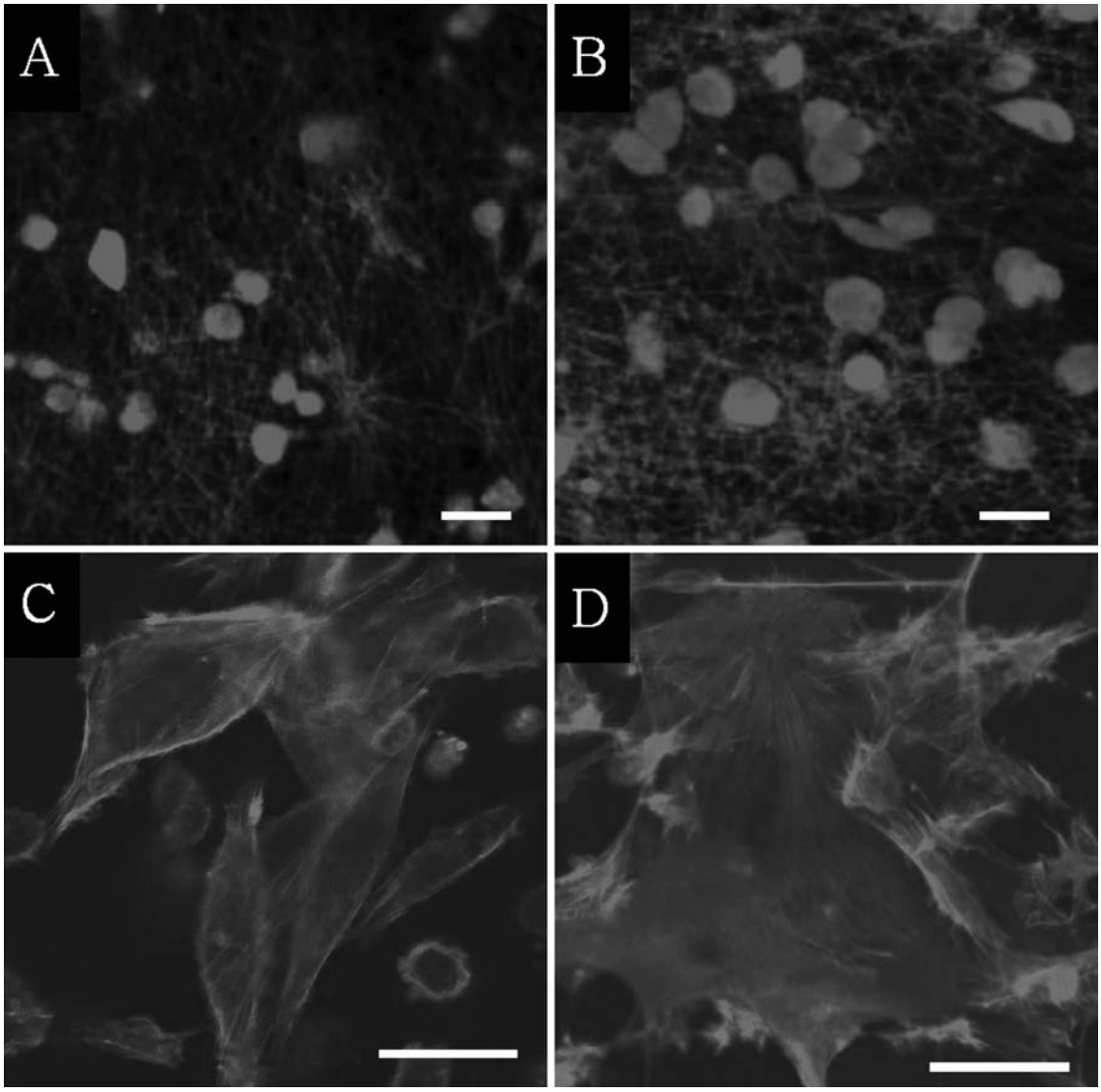

FIG. 7. LSCM images of NIH3T3 fibroblasts on PLGA mesh at 2 and 12 h **(A and C)** and on RGD-immobilized PLGA mesh at 2 and 12 h **(B and D).** Cells were stained with CellTracker **(A and B)** and with rhodamine phalloidin for actin **(C and D).** scale bar, 20 μm

higher stability, nonimmune response, and the ability of selective adhesion of a particular cell type.[39] Numerous polymeric matrices have been immobilized with RGD for enhancing cell-polymer interactions. The RGD peptide has been covalently attached to the surface of polymeric foams, films, hydrogels, and fabrics for using tissue-engineering scaffolds and implanted devices.[21,22,40] RGD-immobilized nonwoven polyester fabrics have been used to cultivate human skin fibroblast in the serum-free medium.[21] These surface-engineered fabrics showed effective cell adhesion and proliferation and also showed high cell densities because of their higher surface area-volume ratio than that in the unmodified substrates. Recently, we have reported that adult stem cells seeded within RGD-modified PLGA porous scaffolds showed promotion in cellular functions.[22] From this perspective, we immobilized RGD peptides to the electrospun nanofibrous mesh for enhancing the cytocompatibility of biodegradable polymers.

In order to introduce surface amine functional groups to the fiber mesh, PLGA-*b*-PEG-NH_2 was blended with PLGA and then hydrated in water. During the hydration, molecular migration and rearrangement of PLGA-*b*-PEG-NH_2 could occur toward the surface of nanofibers, exposing amine functional groups to the aqueous phase. Our previous studies demonstrated that when blending

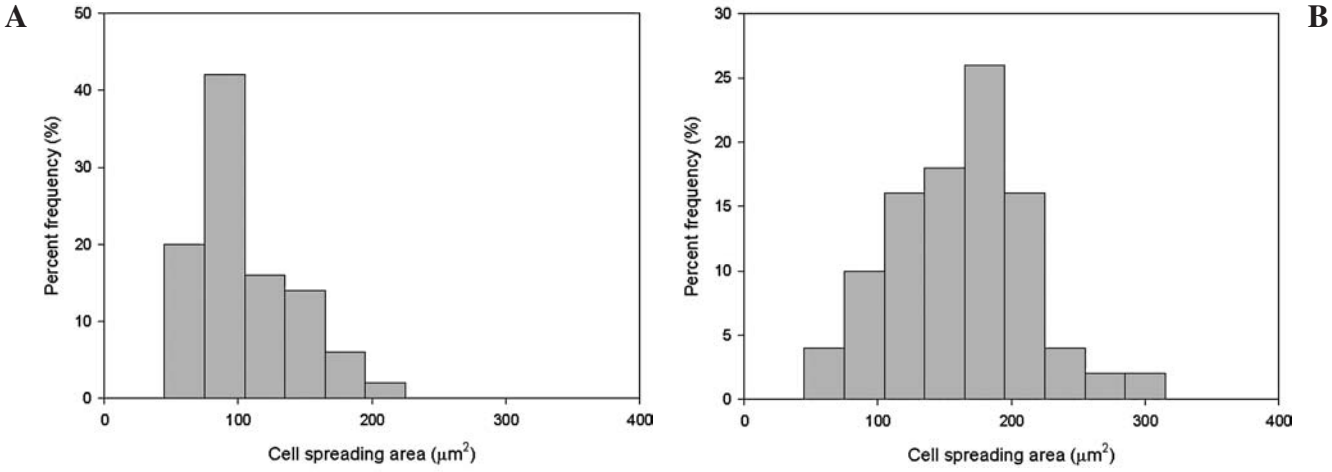

FIG. 8. The distribution of cell-spreading areas on PLGA mesh **(A)** and on RGD-immobilized PLGA mesh **(B)** after 2 h.

PLGA-*b*-PEG-NH_2 with PLGA, the amino groups were exposed on the surface of PLGA scaffolds.[22] Various cell recognizable ligands, such as RGD peptide, galactose, and hyaluronic acid, were grafted to the exposed amino groups on the surface of porous PLGA scaffolds for tissue engineering.[41,42] With surface functional amino groups, GRGDY peptide was covalently conjugated on the surface by NHS-activated coupling reaction. The colorimetric quantification data verified the presence of immobilized RGD on the surface of the mesh. In the water contact angle measurement, the blended mesh showed rapid penetration of a water drop into the mesh, revealing that the blending of PLGA-*b*-PEG-NH_2 indeed increased the wettability of the nanofiber mesh. The surface charge, wettability, and topography influence the cell adhesion process to vastly different extents. In serum-free conditions, it was reported that positively charged surface functional groups enhanced cell attachment.[43]

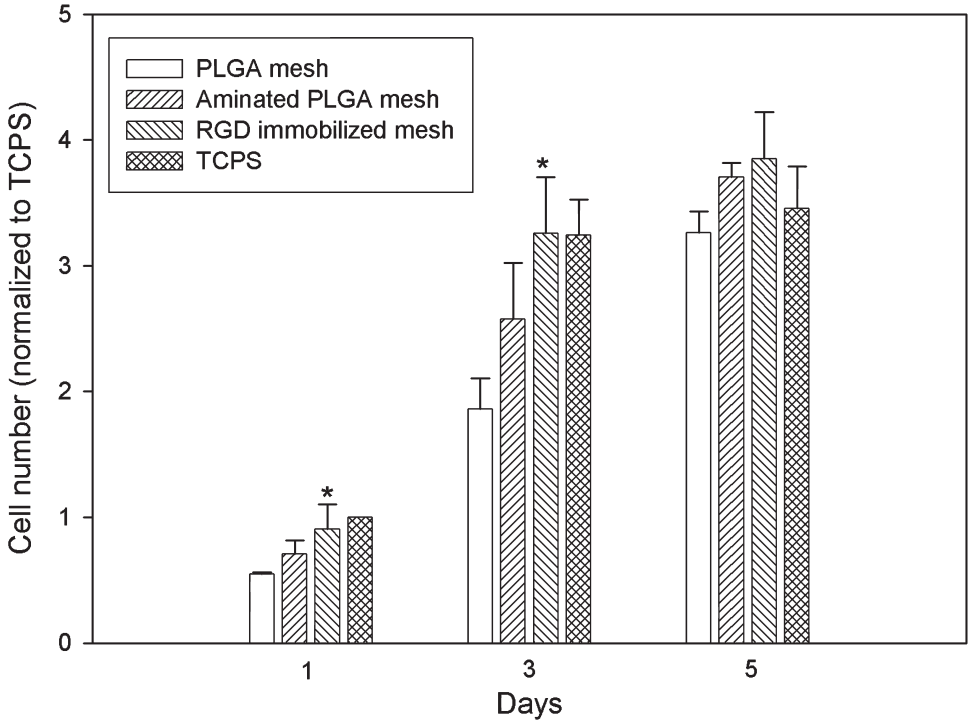

FIG. 9. Cell proliferation on PLGA, aminated PLGA, RGD-immobilized mesh, and TCPS. The cell number was normalized to TCPS at day 1. All values are mean ± SD ($n = 5$). *Statistical significance relative to aminated PLGA mesh ($p < 0.05$).

The present results revealed that the cell attachment in the absence of serum protein was boosted according to the following order: PLGA < aminated PLGA < RGD-modified mesh. PEG is known to show nonadhesive, repelling properties toward proteins and cells. The increased cell attachment for the aminated PLGA mesh relative to PLGA mesh indicates that the hydrophilic nature of PEG block and cationic amino group at the distal end of PEG overwhelmed the nonadhesive effect of the PEG chain. For RGD-modified meshes, immobilized RGD moieties further improved cell adhesion through specific cell-polymer interactions. Enhanced cell spreading and formation of actin fibers in cells on the RGD-immobilized mesh were visualized by SEM and LSCM. The SEM images show that the nanofibrous mesh provided the cells with an ability of morphological change responding to surface topography. Each fiber was easily lifted by contracting force of a single cell. This may be advantageous for cell infiltration since the initial pore diameter in the mesh is too small compared to the size of cells. The improved cell-substrate interaction was confirmed again by measuring the cell-spreading area. In the current study, the organization of the actin cytoskeleton stained by rhodamine phalloidin was qualitatively investigated in order to evaluate the response of fibroblasts to RGD-immobilized fibrous environment. While the cells on the PLGA mesh show diffusive actin staining, prominent stress fibers were apparent on the RGD-immobilized mesh. This implies that the grafted RGD peptides interacted with the cells with concurrently increasing cell spreading. Initial cellular attachment and spreading events, which were mediated by the specific interactions between the immobilized RGD and cell receptors, led to better cell adhesion and proliferation. In the cell proliferation experiment, RGD immobilization on electrospun nanofibrous mesh exhibited the long-term maintenance of cell-substrate interactions. The number of cells proliferated on the RGD-immobilized mesh was significantly higher than those on the other meshes in an early incubation stage, but it became statistically indifferent for the various substrates at day 5. As mentioned above, this might be caused by a contact inhibition mechanism. Cells spread and proliferate up to the formation of monolayer on the polymer surfaces, at which time the cell proliferation is spatially inhibited. Thus it is reasonable to say that there were no differences in cell proliferation in the later stage, regardless of RGD modification on the two-dimensional surface. Finally, it was recently reported that the cells could migrate into nanofibrous mesh having pores less than 10 μm in diameter on the surface.[44,45] Cellular penetration into the nanofibrous scaffolds, however, is still limited because the electrospun nanofibrous meshes have a highly packed structure with pores of less than a few micrometers. To resolve this problem, three-dimensional macroporous scaffolds made from RGD grafted PLGA nanofibrous mesh, which affords sufficient cell seeding within the macropores, are under development and will be reported in the near future.

CONCLUSIONS

In this study, we first demonstrated immobilization of RGD peptides on the electrospun PLGA nanofibrous mesh. Functional amino groups were introduced on the surface of nanofiber by electrospinning a blend mixture of PLGA and PLGA-*b*-PEG-NH_2 di-block copolymer, followed by conjugation with GRGDY peptides. The RGD-immobilized mesh exhibited enhanced cell adhesion, spreading, and proliferation. Our results suggest nanofibrous constructs combined with surface engineering will have great potential for a wide array of cell-contacting biomedical devices, such as tissue-engineering scaffolds, wound dressing materials, and prosthetic devices.

ACKNOWLEDGMENTS

This study was supported by Grant KRF-2004-005-D00070 from the Korea Research Foundation, and the Polymer Technology Institute, Sungkyunkwan University, Korea.

REFERENCES

1. Kim, B.-S., and Mooney, D.J. Development of biocompatible synthetic extracellular matrices for tissue engineering. Trends Biotechnol. **16,** 224, 1998.
2. Hubbell, J.A. Materials as morphogenetic guides in tissue engineering. Curr. Opin. Biotech. **14,** 551, 2003.
3. von Recum, A.F., Shannon, C.E., Cannon, C.E., Long, K.J., and van Kooten, T.G. Surface roughness, porosity, and texture as modifiers of cellular adhesion. Tissue Eng. **2,** 1996, 241.
4. Flemming, R.G., Murphy, C.J., Abrams, G.A., Goodman, S.L., and Nealey, P.F. Effects of synthetic micro- and nano-structured surfaces on cell behavior. Biomaterials **20,** 573, 1999.
5. Karp, G. Cell and molecular biology: concepts and experiments. NY: John Wiley & Sons, 1996, pp. 249–250.
6. Huang, Z.-M., Zhang, Y.-Z., Kotaki, M., and Ramakrishna, S. A review on polymer nanofibers by electrospinning and their application in nanocomposites. Compos. Sci. Technol. **63,** 2223, 2003.
7. Alberto-Rincon, M.C., Zorn, T.M.T., and Abrahamsohn, P.A. Diameter increase of collagen fibrils of the mouse endometrium during decidualization. Dev. Dyn. **186,** 417, 1989.

8. Li, W.-J., Laurencin, C.T., Caterson, E.J., Tuan, R.S., and Ko, F.K. Electrospun nanofibrous structure: a novel scaffold for tissue engineering. J. Biomed. Mater. Res. **60,** 613, 2002.
9. Mo, X.M., Xu, C.Y., Kotaki, M., and Ramakrishna, S. Electrospun P(LLA-CL) nanofiber: a biomimetic extracellular matrix for smooth muscle cell and endothelial cell proliferation. Biomaterials **25,** 1883, 2004.
10. Min, B.M., You, Y., Kim, J.M., Lee, S.J., and Park, W.H. Formation of nanostructured poly(lactic-co-glycolic acid)/chitin matrix and its cellular response to normal human keratinocytes and fibroblasts. Biomaterials **57,** 285, 2004.
11. Yoshimoto, H., Shin, Y.M., Terai, H., and Vacanti, J.P. A biodegradable nanofiber scaffold by electrospinning and its potential for bone tissue engineering. Biomaterials **24,** 2077, 2003.
12. Bhattarai, S.R., Bhattarai, N., Yi, H.K., Hwang, P.H., Cha, D.I. and Kim, H.Y. Novel biodegradable electrospun membrane: scaffold for tissue engineering. Biomaterials **25,** 2595, 2004.
13. Hollinger, J.O., and Battistone, G.C., Biodegradable bone repair materials: synthetic polymers and ceramics. Clin. Orthop. Rel. Res. **207,** 290, 1986.
14. Iwan, Z., Dietmar, W.H., Kim, C.T., and Swee, H.T. Fused deposition modeling of novel scaffold architectures for tissue engineering applications Biomaterials **23,** 1169, 2002.
15. Nam, Y.S., Yoon, J.J., and Park, T.G. A Novel fabrication method for macroporous scaffolds using gas foaming salt as porogen additive. J. Biomed. Mater. Res. **53,** 1, 2000.
16. Glass, J.R., Dickerson, K.T., Stecker, K., and Polarek, J.W. Characterization of a hyaluronic acid-Arg-Gly-Asp peptide cell attachment matrix. Biomaterials **17,** 1101, 1996.
17. Lebaron R.G., and Athanasiou K.A. Extracellular matrix cell adhesion peptides: functional application orthopedic materials. Tissue Eng. **6,** 85, 2000.
18. Chen, C.S., Mrksich, M., Huang, S., Whitesides, G.M., and Ingber D.E. Geometric control of cell life and death. Science **276,** 1425, 1997.
19. Cook, A.D., Hrkach, J.S., Gao, N.N., Johnson, I.M., Pajvani, U.B., Cannizzaro, S.M., and Langer, R. Characterization and development of RGD-peptide-modified poly(lactic acid-co-lysine) as an interactive, resorbable biomaterial. J. Biomed. Mater. Res. **35,** 513, 1997.
20. Yamaoka, T., Hotta, Y., Kobayashi, K., and Kimura, Y., Synthesis and properties of malic acid-containing functional polymers. Int. J. Biol. Macromol. **25,** 265, 1999.
21. Gümü-derelio-lu, M., and Türko-lu, H. Biomodification of non-woven polyester fabrics by insulin and RGD for use in serum-free cultivation of tissue cells. Biomaterials **23,** 3927, 2002.
22. Yoon, J.J., Song, S.H., Lee, D.S., and Park, T.G. Immobilization of cell adhesive RGD onto the surface of highly porous biodegradable polymer scaffolds fabricated by a gas foaming/salt leaching method. Biomaterials **25,** 5613, 2004.
23. Kenawy, E.-R., Bowlin, G.L., Mansfield, K., Layman, J., Simpson, D.G., Sanders, E.H., and Wnek, G.E. Release of tetracycline hydrochloride from electrospun poly(ethylene-co-vinylacetate), poly(lactic acid), and a blend. J. Control. Release **81,** 57, 2002.
24. Katti, D.S., Robinson, K.W., Ko, F.K., and Laurencin, C.T. Bioresorbable nanofiber-based systems for wound healing and drug delivery: optimization of fabrication parameters. J. Biomed. Mater. Res. **70,** 286, 2004.
25. Zong, X., Kim, K., Fang, D., Ran, S., Hsiao, B.S., and Chu, B. Structure and process relationship of electrospun bioabsorbable nanofiber membranes. Polymer **43,** 4403, 2002.
26. Zhang, Q., Wang, C., Babukutty, Y., Ohyama, T., Kogoma, M., and Kodama, M. Biocompatibility evaluation of ePTFE membrane modified with PEG in atmospheric pressure glow discharge. J. Biomed. Mater. Res. **60,** 502, 2002.
27. Isobe, I., Michikawa, M., and Yanagisawa, K. Enhancement of MTT, a tetrazolium salt, exocytosis by amyloid b-protein and chloroquine in cultured rat astrocytes. Neurosci. Lett. **266,** 129, 1999.
28. McDevitt, T.C., Woodhouse, K.A., Hauschka, S.D., Murry, C.E., and Stayton, P.S. Spatially organized layers of cardiomyocytes on biodegradable polyurethane films for myocardial repair. J. Biomed. Mater. Res. **66A,** 586, 2003.
29. Deitzel, J.M., Kleinmeyer, J., Harris, D., and Tan, N.C.B. The effect of processing variables on the morphology of electrospun nanofibers and textiles. Polymer **42,** 261, 2001.
30. Kim, K.S., Yu, M., Zong, X., Chiu, J., Fang, D., Seo, Y.S., Hsiao, B.S., Chu, B., and Hadjiargyrou, M. Control of degradation rate and hydrophilicity in electrospun non-woven poly(D,L-lactide) nanofiber scaffold for biomedical applications. Biomaterials **24,** 4977, 2003.
31. Kwon, Y.J., and Peng, C.A. Impact of cell growth morphology on retroviral transduction: Effect of contact inhibition. Biotechnol. Prog. **17,** 240, 2001.
32. Kim, J., and Reneker, D.H. Mechanical properties of composites using ultrafine electrospun fibers. Polym. Composites **20,** 124, 1999.
33. Frenot, A., and Chronakis, I.S. Polymer nanofibers assembled by electrospinning. Curr. Opin. Colloid Interf. Sci. **8,** 64, 2003.
34. Ranucci, C.S., and Moghe, P.V. Substrate microphotography can enhance cell adhesive and migratory responsiveness to matrix ligand density. J. Biomed. Mater. Res. 54, 149, 2001.
35. Teixeira, A.I., Nealey, P.F., and Murphy, C.J. Responses of human keratocytes to micro- and nanostructured substrates. J. Biomed. Mater. Res. **71A,** 369, 2004.
36. Curtis, A., and Wilkinson, C. Topographical control of cells. Biomaterials **18,** 1573, 1997.
37. Guidoin, R., Marceau, D., Couture, J., Rao, T.J., Merhi, Y., Roy, P.E., and De la Faye, D. Collagen coatings as biological sealants for textile arterial prostheses. Biomaterials **10,** 156, 1989.
38. Dean, J.W., Culbertson, K.C., and D'Angelo, A.M. Fibronectin and laminin enhance gingival cell attachment to dental implant surfaces in vitro. Int. J. Oral. Max. Impl. **10,** 721, 1995.
39. Hersel, U., Dahmen, C., and Kessler, H. RGD modified polymers: biomaterials for stimulated cell adhesion and beyond. Biomaterials **24,** 4385, 2003.
40. Woerly, S., Pinet, E., de Robertis, L., Van Diep, D., and Bousmina, M. Spinal cord repair with PHPMA hydrogel containing RGD peptides (NeuroGel). Biomaterials **22,** 1095, 2001.
41. Park, T.G. Perfusion culture of hepatocytes within galactose-derivatized biodegradable poly(lactide-co-glycolide)

scaffolds prepared by gas foaming of effervescent salts. J. Biomed. Mater. Res. **59,** 127, 2002.
42. Yoon, J.J., Nam, Y.S., Kim, J.H., and Park, T.G. Surface immobilization of galactose onto aliphatic biodegradable polymers for hepatocyte culture. Biotech. Bioeng. **78,** 1, 2002.
43. Griesser, H.J., Chatelier, R.C., Gengenbach, T.R., Johnson, G., and Steele, J.G. Growth of human cells on plasma polymers: putative role of amine and amide groups. J. Biomat. Sci. Polym. Edn. **5,** 531, 1994.
44. Zhang, Y., Ouyang, H., Lim, C.T., Ramakrishna, S., and Huang, Z.M. Electrospinning of gelatin fibers and gelatin/PCL composite fibrous scaffolds. J. Biomed. Mater. Res. **72B,** 156, 2005.
45. Khil, M.S., Bhattarai, S.R., Kim, H.Y., Kim, S.Z., and Lee, K.H. Novel fabricated matrix via electrospinning for tissue engineering. J. Biomed. Mater. Res. **72B,** 117, 2005.

Address reprint requests to:
Tae Gwan Park, Ph.D.
Department of Biological Sciences
Korea Advanced Institute of Science and Technology
Daejeon 305-701
South Korea

E-mail: tgpark@kaist.ac.kr